ARTICLE

BIOTECHNOLOGY and BIOENGINEERING

Protein Products Obtained by Site-Preferred Partial Crosslinking in Protein Crystals and "Liberated" by Redissolution

Michal Buch,[1] Yariv Wine,[1] Yael Dror,[1] Sonia Rosenheck,[1] Mario Lebendiker,[2] Rita Giordano,[3] Ricardo M.F. Leal,[4] Alexander N. Popov,[5] Amihay Freeman,[1] Felix Frolow[1,6]

[1]Department of Molecular Microbiology and Biotechnology, Tel Aviv University, 69978, Tel-Aviv, Israel; telephone: +972-36409054; fax: +972-36405147; e-mail: amihayf@post.tau.ac.il

[2]Protein Purification Facility, Wolfson Center, The Hebrew University of Jerusalem, Jerusalem, Israel

[3]Swiss Light Source at Paul Scherrer Institute, Villigen, Switzerland

[4]ESRF, Grenoble, France

[5]ILL, Grenoble, France

[6]The Daniella Rich Institute for Structural Biology, Tel Aviv University, 69978, Tel Aviv, Israel

ABSTRACT: The use of protein crystals as a source of nanoscale biotemplates has attracted growing interest in recent years owing to their inherent internal order. As these crystals are vulnerable to environmental changes, potential applications require their stabilization by chemical crosslinking. We have previously shown that such intermolecular chemical crosslinking reactions occurring within protein crystals are not random events, but start at preferred crosslinking sites imposed by the alignment of protein molecules and their packing within the crystalline lattice. Here we propose a new working hypothesis and demonstrate its feasibility in enabling us to extricate homogeneous populations of single protein molecules that display chemical point mutations or of dimers that show homogeneous chemical crosslinking, and that have the potential for isolation of higher structures. Characterization of the crosslinking mechanism and its end products opens the way to the potential retrieval of such specific modified/intermolecular crosslinked products simply by effecting partial crosslinking at identified preferred sites, followed by time-controlled arrest of the crosslinking reaction and dissolution of the crystals by medium exchange complemented by chromatographic purification.

Correspondence to: A. Freeman and F. Frolow
Contract grant sponsor: Israel Science Foundation (ISF)
Contract grant number: 839/08
Contract grant sponsor: Edouard Seroussi Chair for Protein Nano-Biotechnology
Received 12 October 2013; Revision received 29 December 2013; Accepted 3 January 2014
Accepted manuscript online xx Month 2014
Article first published online in Wiley Online Library (wileyonlinelibrary.com).
DOI 10.1002/bit.25186

Biotechnol. Bioeng. 2014;9999: 1–8.

KEYWORDS: protein crystals; crosslinking; glutaraldehyde; X-ray diffraction; structure analysis

Introduction

Protein crystals that are routinely prepared for elucidation of protein 3D structure by X-ray crystallography present a highly ordered 3D array of protein molecules. In addition, formed along with this molecular array is a complementary 3D array of voids, consisting of solution-filled cavities and interconnecting channels whose pattern, geometry, and size depend on the protein molecule dimensions, shape, and intermolecular interactions. These intermolecular interactions are dictated in turn by the composition of the surfaces of the protein molecules (Cohen-Hadar et al., 2006, 2009). The void volume, the space that is occupied by the solvent and is responsible for the definition of porosity of the protein crystal, varies between 30% and 70% of crystal's total volume (Matthews, 1968).

The porosity of protein crystals, which enables them to be permeated by low-molecular-weight solutes, has been exploited for their use in enzyme-mediated organic synthesis (Margolin and Navia, 2001; Zelinski and Waldmann, 1997) and size-exclusion chromatography (Vilenchik et al., 1998). As a prerequisite for such applications, it was necessary to stabilize the vulnerable protein crystals to changing environments by chemical crosslinking of neighboring protein

molecules embedded within the crystal. This was done by the use of bifunctional or multifunctional crosslinking agents, such as glutaraldehyde (Margolin and Navia, 2001; Zelinski and Waldmann, 1997). In addition to the above-mentioned applications, stabilization of protein crystals by glutaraldehyde crosslinking also enables them to be used as biotemplates, as demonstrated by the use of glutaraldehyde-stabilized concanavalin A crystals as a biotemplate for fabrication of a 3D array of metallic silver nanoparticles embedded within the internal crystalline voids. This could be achieved either by directed electroless deposition (Cohen-Hadar et al., 2009) or by photoreduction of periodically deposited silver ions in the solvent channels of glutaraldehyde-crosslinked lysozyme crystals (Guli et al., 2010).

Elucidation of the end products and the molecular mechanism underlying protein crystal crosslinking by glutaraldehyde was previously described by our laboratory (Wine et al., 2007). Structural analysis by X-ray diffraction of lysozyme crystals crosslinked by glutaraldehyde for longer than 24 h under acidic (pH 4.8) or alkaline (pH 8.0) conditions revealed site-preferred crosslinking of lysine13 residues of neighboring lysozyme molecules. Under acidic conditions the reaction rate was much slower, and the result was that bridging of the same two lysine13 residues of neighboring lysozyme molecules culminated in a different crosslinking end product. It was observed in that study that chemical crystal crosslinking involves a specific initiation site for preferable crosslinking, presumably indicating that it is ``guided'' by the alignment of protein molecules throughout the crystallization process so that some of their amino acid residues are displayed close to neighboring molecules in the crystal's pores, readily accessible to low-molecular-weight crosslinking agents.

On the basis of this mechanism we now propose a working hypothesis that provides a new tool for the preparation of homogeneous populations of protein molecules modified at specific sites or protein dimers of protein molecules, all crosslinked through the same specific site, or of higher protein arrays obtained by using a series of site-preferred crosslinking reactions effected by several different chemical crosslinking agents. Such chemically modified or crosslinked homogeneous protein populations may be readily extricated by the arrest of site-preferred crosslinking reactions achieved through washing with crystallization medium devoid of the crosslinking agent, followed by medium exchange that brings about crystal dissolution.

In this study we demonstrated the feasibility of our ``extrication'' working hypothesis by preparing (i) a homogeneous population of protein molecules displaying identical chemical point mutations, and (ii) a homogeneous population of chemically crosslinked protein dimers all crosslinked via the same residues.

Materials and Methods

Preparation of Crosslinked Crystals

Lyophilized hen egg white lysozyme (HEWL, Sigma, St. Louis, MO) was dissolved to a concentration of 50 mg/mL in 3 mL of 0.1 M sodium acetate pH 4.8 and transferred into three tubular dialysis membranes (MWCO 6000–8000, CelluSep, Seguin, TX). The enzyme solutions were dialyzed (1:100 v/v) against 3.5% NaCl in 0.1 M sodium acetate pH 4.8. Following overnight incubation at 18°C the crystals were transferred into separate test tubes and washed three times with 5 mL of the crystallization solvent (3.5% NaCl in 0.1 M sodium acetate pH 4.8). Crosslinking was carried out by incubating the crystals in solution, consisting of 0.1 M sodium acetate pH 4.8, 3.5% NaCl, and 1% (v/v) glutaraldehyde (Merck, Darmstadt, Germany) for 10 min, 24 or 48 h. The crosslinking reaction was arrested by medium exchange followed by washing three times with crystallization solvent devoid of glutaraldehyde.

Purification of Partially Crosslinked Crystal End Products by Ion Exchange Chromatography

HEWL crystals were grown in the dialysis bags and crosslinked for 10 min as described above. The crosslinker was then removed by washing the partially crosslinked crystals with crystallization solution, and crystals were dissolved by replacement of buffer with 0.1 M sodium acetate pH 4.8. Samples of the dissolved crystals were loaded on 15S cation-exchange columns (FPLC system, ÄKTAexplorer, GE Healthcare, Piscataway, NJ). Protein fractions were eluted from the column at a flow rate of 1.5 mL/min by applying a stepwise gradient of sodium chloride (0–0.4 M) in 20 mM HEPES pH 7.0. Elution was monitored by UV absorption at $\lambda = 280$ nm.

Following the chromatographic procedure, fractions containing lysozyme monomers or dimers were combined, desalted, and concentrated to at least 30 mg/mL using a Centricon centrifugal filter (3000 MWCO, Millipore, MA).

Mass Spectrometry

Mass spectrometric analysis was performed using the QSTAR® XL Hybrid LC/MS/MS (Applied BioSystems, Foster City, CA) nano-electrospray ionization system.

SDS–PAGE

Sodium dodecyl sulfate–polyacrylamide gel electrophoresis (SDS–PAGE) was carried out with a Mini-PROTEAN® 3 system (Biorad, Hercules, CA) consisting of a 12.5% polyacrylamide gel and a 4% polyacrylamide stacking gel.

Residual Enzymatic Activity

The residual lysozyme hydrolytic activity of isolated and purified monomers and dimers was determined using insoluble suspended substrate (cell wall of *Micrococcus lysodeikticus* after Worthington, 1993) and soluble substrate (PNP-$(GlcNAc)_3$-β-*N*-acetylglucosaminidase coupled assay after Nanjo et al., 1988).

Crystallization of Chromatographically Purified Lysozyme Monomers and Dimers

Glutaraldehyde-modified and chromatographically purified lysozyme monomers were crystallized by the hanging drop vapor diffusion technique and purified glutaraldehyde-crosslinked lysozyme dimers crystallization was conducted by using the microbatch-under-oil method (Ducruix and Giege, 1999). Modified lysozyme monomer crystals were grown from protein solution (30 mg/mL, 0.1 M sodium acetate pH 4.8) mixed to a 1:1 ratio (4 μL each) with precipitant solution (3–9% NaCl in 0.1 M sodium acetate pH 4.8) and equilibrated at 18°C over 0.4 mL of the precipitating solution. Crystallization conditions for the crosslinked lysozyme dimers were screened using a Crystal Screen HT (Hampton Research, Aliso Viejo, CA) in a 96-well micro-batch plate (1 μL of 5 mg/mL protein solution and 1 μL precipitant). Screening was performed at 18°C with an Oryx6 crystallization robot (Douglas Instruments, Berkshire, UK).

Diffraction Experiments and Structure Refinement

Twenty representative crystals were selected from the three time-groups of crosslinked lysozyme crystals: ten crystals crosslinked for 10 min, five crosslinked for 24 h, and five crosslinked for 48 h. Each crosslinked crystal was harvested from the crystallization solvent and transferred into cryoprotectant solution (0.1 M sodium acetate pH 4.8, 3.5% NaCl and 25% ethylene glycol) using CryoLoop™ (Teng, 1990). The crystals were immediately plunged into liquid nitrogen and put in pucks to transport to synchrotron for data collection (ESRF, Grenoble, France). The crystals were placed in a stream of cold nitrogen at a temperature of 100 K, which was generated by Oxford Cryosystems (Cosier and Glazer, 1986). Diffraction data sets were indexed, integrated, and scaled using DENZO and SCALEPACK as implemented by HKL2000 (Otwinowski and Minor, 1997), and by using the programs XDS and XSCALE (Kabsch, 1993; Kabsch, 2010a,b). Structures were refined and electron-density maps calculated (2Fobs-Fcalc and Fobs-Fcalc) by the use of PHENIX software (Adams et al., 2010), with 5% of the total data excluded from the refinement for the purpose of R_{free} calculations. Structures were rebuilt and validated using COOT (Emsley et al., 2010), and molecular images were rendered using PyMOL software (DeLano, 2002).

Results and Discussion

Short-Term Versus Long-Term Glutaraldehyde Crosslinking of Lysozyme Crystals and Crystal Dissolution

Tetragonal HEWL crystals crosslinked by incubation in 1% (v/v) glutaraldehyde solution for 10 min, 24 or 48 h were dissolved by incubation in 0.1 M sodium acetate pH 4.8 and the resulting solutions were analyzed by SDS–PAGE. The results described in Figure 1 showed that dimerization had already occurred by 10 min after the start of the crosslinking

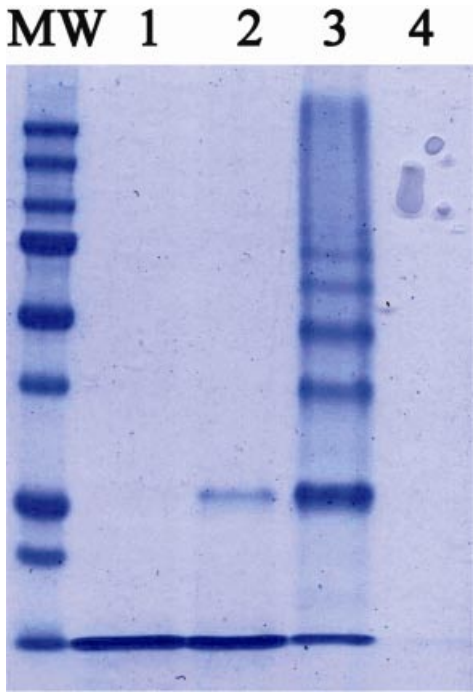

Figure 1. SDS–PAGE analysis. **Lane 1**: dissolved native crystals; **lanes 2–4**: dissolved crystals crosslinked with 1% (v/v) glutaraldehyde for 10 min (lane 2), for 24 h (lane 3), and for 48 h (lane 4). MW: low-molecular-weight protein marker.

reaction. Unlike the complete dissolution of crystals crosslinked for 10 min, crystals that were crosslinked for 24 h were largely resistant to dissolution, releasing less than 10% of their volume to the dissolution buffer and revealing mostly crosslinked dimers and higher crosslinking products. Attempts to dissolve crystals that were crosslinked for 48 h failed, indicating that these crystals had become fully resistant to dissolution.

To gain further insight into the potential impact of the crosslinking reaction on protein alignment within the partially crosslinked (10 min) or fully crosslinked lysozyme crystals (24 and 48 h), we analyzed the X-ray diffraction of representative groups of crystals incubated for 10 min, 24 or 48 h, and then performed statistical calculations of hierarchical clustering on the collected data sets to determine the degree of isomorphism between the crosslinked crystals representing each group. According to hierarchical clustering method (Giordano et al., 2012), a correlation-coefficient matrix was calculated for the intensities that were scaled but not merged for each pair of data sets. This matrix was then used to define an isomorphism distance criterion, for estimation of the structural similarity between the crystals.

Results obtained from the hierarchical cluster analysis (Fig. 2) depict two main clusters, one containing data sets from crystals crosslinked for 10 min and the other containing data sets from crystals crosslinked for 24 and 48 h. Each of the main clusters was further divided into two sub-clusters. Whereas crystals crosslinked for 10 min exhibited two sub-

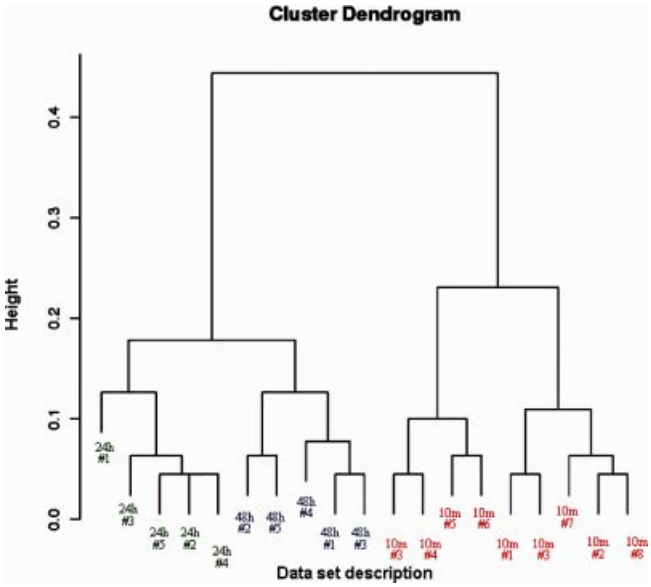

Figure 2. Hierarchical cluster analysis dendrogram for 18 data sets of crosslinked lysozyme crystals (eight crosslinked for 10 min (red); five crosslinked for 24 h (green); and five crosslinked for 48 h (blue)). The *Y*-axis defines the distance between the clusters.

clusters, data sets obtained for crystals crosslinked for 24 and 48 h each appeared as separate sub-cluster. These findings point to a significant structural difference between the 10-min data sets and the 24 or 48-h data sets, indicating a higher degree of similarity among the 24 and 48-h data sets, in accord with their observed resistance to dissolution, than in the 10-min data sets, which were found to be hierarchically more divergent.

Structural Analysis of Crosslinked Lysozyme Crystals

Electron-density maps were calculated from 20 structures of lysozyme crystals crosslinked for 10 min, 24 and 48 h. Standard data-processing statistics are summarized in Tables I and II. The refined models revealed specific regions of extended electron densities that appeared repetitively throughout the crystal lattice of the different time-groups of crosslinked crystals. In the ten 10-min-crosslinked crystals that we examined, a distinctive electron-density continuum was unexpectedly observed between two *N*-guanidyls of Arg45 from two neighboring lysozyme molecules related by a crystallographic twofold axis (see Fig. 3b). On the other hand, in the 24 and 48-h-crosslinked crystal models (5 crystals each) an additional electron-density continuum was identified, connecting the two ε-amines of Lys13 from two adjacent lysozyme molecules (Fig. 3c and e).

These sequential time-dependent crosslinking reactions utilizing two different preferred crosslinking sites resulted in fast crosslinking of Arg45–Arg45 complemented by the much slower secondary crosslinking reaction of Lys13–Lys13, enabling us to potentially extricate lysozyme dimers resulting

Table I. Crystal parameters and data collection statistics for data sets of lysozyme crystals crosslinked for 10 min.

Data set	10 min #1	10 min #2	10 min #3	10 min #4	10 min #5	10 min #6	10 min #7	10 min #8	10 min #9	10 min #10
Space group	$P4_32_12$	$P4_32_12$	$P4_32_12$	$P4_32_12$	$P4_32_12$	$P4_32_12$	$P4_32_12$	$P4_32_12$	$P4_32_12$	$P4_32_12$
Unit cell parameters (Å)	$a=b=78.804$, $c=36.950$	$a=b=78.494$, $c=36.849$	$a=b=78.542$, $c=36.927$	$a=b=78.673$, $c=36.909$	$a=b=78.515$, $c=36.946$	$a=b=78.410$, $c=36.795$	$a=b=78.451$, $c=36.934$	$a=b=78.599$, $c=36.819$	$a=b=78.618$, $c=36.862$	$a=b=78.526$, $c=36.885$
Unit cell volume (Å^3)	229461.3	227043.9	227792.6	228446.7	227756.5	226220.9	227316.4	227458.3	227834.5	227447.4
Resolution range (Å)	30.0–1.25	50.0–1.21	30.0–1.32	30.0–1.35	30.0–1.42	50.0–1.21	50.0–1.38	50.0–1.38	50.0–1.38	50.0–1.38
No. of reflections	401931	379831	343706	271586	177577	288846	306151	340654	329707	325871
Completeness (%)	99.3 (98.8)	98.8 (84.8)	100.0 (100.0)	99.8 (98.6)	99.2 (97.1)	99.8 (99.5)	99.6 (98.9)	100.0 (100.0)	100.0 (100.0)	99.1 (97.2)
Mosaicity range (°)	0.32–0.72	0.36–0.45	0.41–0.69	0.29–0.71	0.55–0.96	0.49–0.72	0.62–0.86	0.39–0.55	0.39–0.74	0.33–0.39
R_{merge}[a]	0.072	0.054	0.056	0.054	0.040	0.052	0.059	0.055	0.072	0.064
I/σ (I)	36.5 (2.4)	33.9 (1.0)	44.9 (2.4)	36.7 (2.2)	35.2 (1.8)	43.4 (2.1)	38.6 (1.2)	48.0 (3.2)	38.5 (2.2)	33.2 (1.7)

Values in parentheses are for the highest resolution shell.

[a] $R_{merge} = \sum hkl \sum i |I_i(hkl) - I(hkl)| / \sum hkl \sum i I_i(hkl)$, where $\sum hkl$ denotes the sum over all reflections and $\sum i$ the sum over all equivalent and symmetry-related reflections (Stout and Jensen, 1968).

Table II. Crystal parameters and data collection statistics for data sets of lysozyme crystals crosslinked for 24 and 48 h.

Data set	24 h #1	24 h #2	24 h #3	24 h #4	24 h #5	48 h #1	48 h #2	48 h #3	48 h #4	48 h #5
Space group	$P4_32_12$	$P4_32_12$	$P4_32_12$	$P4_32_12$	$P4_32_12$	$P4_32_12$	$P4_32_12$	$P4_32_12$	$P4_32_12$	$P4_32_12$
Unit cell parameters (Å)	$a = b = 78.584$, $c = 36.919$	$a = b = 78.527$, $c = 36.784$	$a = b = 78.556$, $c = 36.741$	$a = b = 78.614$, $c = 36.761$	$a = b = 78.658$, $c = 36.820$	$a = b = 78.469$, $c = 36.784$	$a = b = 78.564$, $c = 36.840$	$a = b = 78.462$, $c = 36.833$	$a = b = 78.458$, $c = 36.769$	$a = b = 78.631$, $c = 36.975$
Unit cell volume (Å^3)	227995.9	226828.1	226733.1	227190.8	227808.9	226492.0	227382.6	226757.3	226338.1	228613.5
Resolution range (Å)	50.0–1.38	50.0–1.38	50.0–1.38	50.0–1.38	50.0–1.38	50.0–1.57	50.0–1.24	50.0–1.38	50.0–1.38	50.0–1.38
No. of reflections	334,007	324,541	334,004	342,727	344,585	232,068	402,998	302379	288566	192550
Completeness (%)	99.7 (95.2)	99.6 (99.7)	100.0 (100.0)	99.8 (97.0)	99.7 (97.8)	100.0 (100.0)	100.0 (99.3)	100.0 (99.9)	100.0 (100.0)	98.7 (97.2)
Mosaicity range (°)	0.27–0.94	0.21–0.41	0.27–0.49	0.20–0.25	0.21–0.27	0.23–0.26	0.14–0.16	0.21–0.40	0.22–0.31	0.16–0.20
R_{merge} [a]	0.042	0.038	0.039	0.035	0.037	0.043	0.057	0.043	0.045	0.038
I/σ (I)	63.2 (3.7)	67.2 (3.1)	71.3 (3.8)	74.3 (5.4)	71.8 (4.2)	61.4 (5.9)	50.3 (7.1)	59.2 (2.6)	62.7 (3.6)	43.8 (4.2)

[a] $R_{merge} = \sum hkl \sum i |I_i(hkl) - I(hkl)| / \sum hkl \sum i I_i(hkl)$, where $\sum hkl$ denotes the sum over all reflections and $\sum i$ the sum over all equivalent and symmetry-related reflections (Stout and Jensen, 1968).

from the first crosslinking reaction indicated by the SDS–PAGE findings. Furthermore, it appears from the crystallographic data presented in Figure 3 that whereas the first crosslinking reaction (Arg45–Arg45, see Fig. 3b) was mediated by a glutaraldehyde ``monomer'' the second crosslinking reaction (Lys13–Lys13, see Fig. 3c and e) was mediated by polymeric glutaraldehyde as described by (Migneault et al., 2004), via the mechanism previously identified by our lab for glutaraldehyde crosslinking effected under acidic pH (see Wine et al., 2007, Fig. 7). The slower rate of the second crosslinking reaction may thus be explained in terms of steric hindrance imposed by the close proximity of the crosslinked lysine residues, brought about by the densely packed lysozyme crystal exhibiting relatively narrow interchannels of 7–23 Å. An additional factor might be that small molecular conformational changes effected by the previous crosslinking of Arg45 residues, as shown in Figure 4a, Leu129 and Lys13 residues in the 10-min-crosslinked crystal (magenta), are involved in a network of salt bridges that draws them closer together, whereas in the 24-h (green) and 48-h (orange) crosslinked crystals (Fig. 4b) these residues are drawn further apart, as reflected by the resulting downwards displacement of the Leu129 residues (shown in Fig. 4c), which probably reflects steric hindrance glutaraldehyde crosslinking impose on neighboring Lys13 ε-amines.

Isolation, Characterization, and Recrystallization of Modified Lysozyme Monomers and Crosslinked Lysozyme Dimers Obtained by Dissolution of Partially Crosslinked Lysozyme Crystals

Purification of Lysozyme Monomers and Dimers Retrieved by Dissolution From Partially (10-min) Crosslinked Lysozyme Crystals

Solution obtained from dissolution of crystals was purified and fractionated by ion-exchange chromatography, yielding separated monomeric and dimeric fractions (Fig. 5a). The two fractions were subjected to electrospray ionization mass spectrometry (ESI-MS) (Fig. 5b), which revealed two major peaks corresponding to lysozyme monomer (Lys-M, 14.309 kDa) and dimer (Lys-D, 28.747 kDa). Deviation from the calculated molecular weight of a lysozyme dimer (28.618 kDa) was small (0.129 kDa), indicating the presence of the glutaraldehyde crosslinker. The minor peaks seen in Figure 5b all over the molecular weight axis imply the presence of polyglutaraldehyde chains of variable lengths attached to monomeric or dimeric lysozyme molecules.

Impact of Crystallization, Crosslinking and Dissolution Process on Residual Enzymatic Activity

The enzymatic activities of dissolved and purified end products Lys-M and Lys-D were assayed using suspended *M. lysodeikticus* cells or the low molecular weight substrate PNP-$(GlcNAc)_3$-β-*N*-acetylglucosaminidase coupled assay (Nanjo et al., 1988). While the residual specific bacteriolytic activities

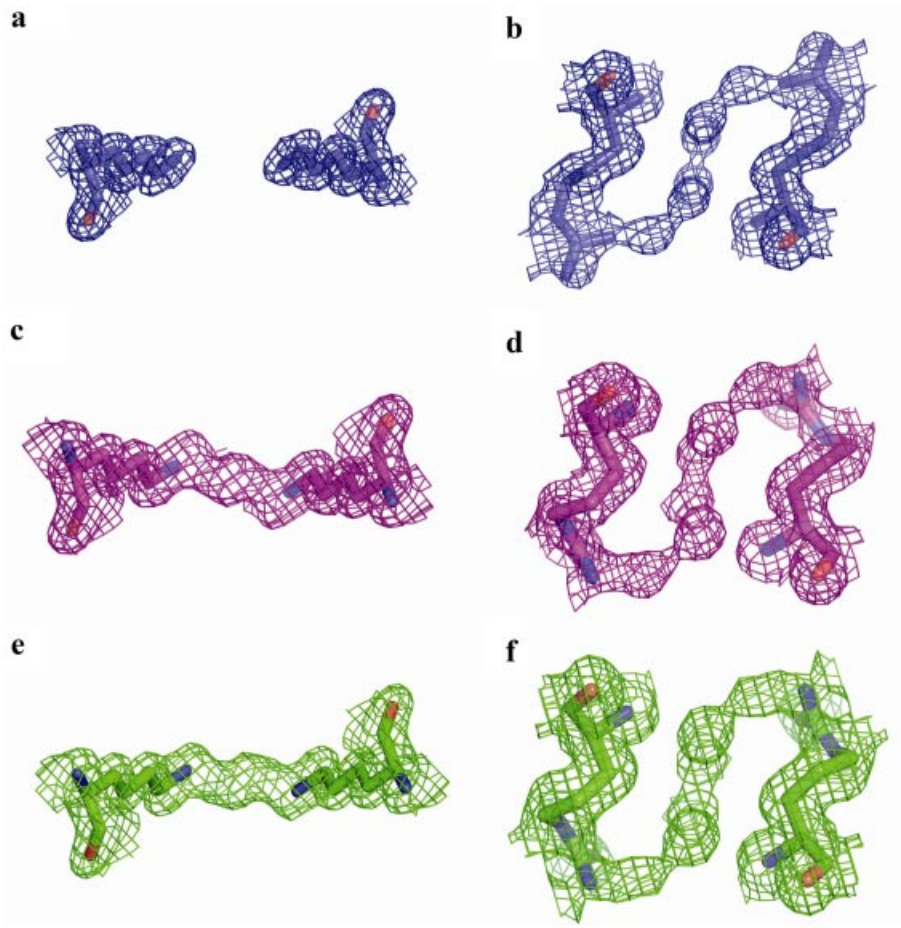

Figure 3. Electron density maps of (**a**, **c**, **e**) Lys13 and (**b**, **d**, **f**) Arg45 crosslinking sites, as depicted in lysozyme crystals crosslinked for 10 min (a, b), for 24 h (c, d), and for 48 h (e, f).

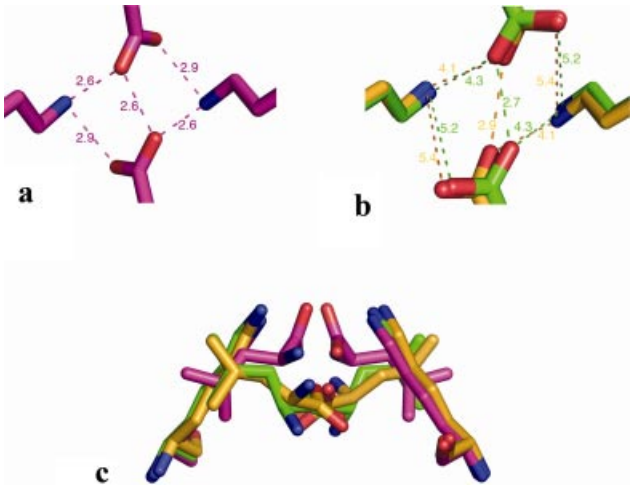

Figure 4. Distance between Lys13 and Leu129 residues in a lysozyme crystal crosslinked (**a**) for 10 min (magenta) and (**b**) for 24 h (green) and 48 h (orange). **c** Superposition of C-terminal region depicting downward displacement of Leu129 residues due to glutaraldehyde crosslinkage in crystals crosslinked for 24 and 48 h.

of both Lys-M and Lys-D were respectively decreased by the process to 82% and 49% of the specific activity exhibited by their parent native enzyme, their specific hydrolytic activities on the soluble substrate have significantly increased respectively to 143% and 172%. It appears that while both lysozyme monomer modification and crosslinking into dimer affected steric hindrance interfering with cell wall lysis, same modifications enhanced the hydrolysis of low molecular weight soluble substrate.

Crystallization of Glutaraldehyde-Modified Monomers of Lysozyme

The modified lysozyme monomeric fraction was readily crystallized using the hanging drop method under similar conditions to those used to crystallize the parent lysozyme (0.1 M sodium acetate pH 4.8 with sodium chloride as precipitant). Crystal parameters and statistics of data collection are listed in Table III. While noticeable intramolecular structural changes were not observed, the complicated electron density appearance observed between the Arg45–Arg45 pair suggested that some of these residues were

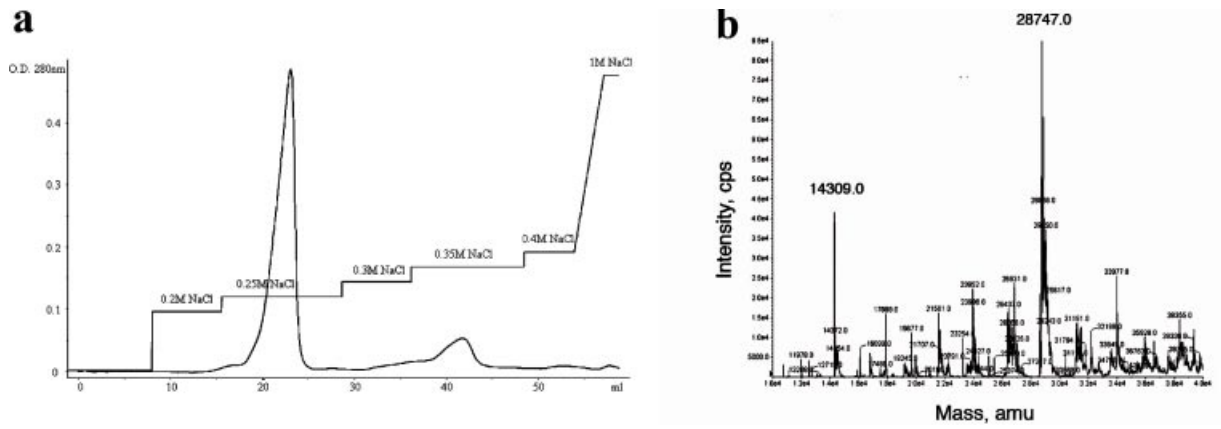

Figure 5. **a**: Ion-exchange elution profile of dissolved crystal products crosslinked for 10 min. **b**: ESI-MS spectrometry of the dimeric fraction retrieved from chromatography.

Table III. Crystal parameters and data collection statistics for the parent lysozyme, the purified modified lysozyme monomer and the purified crosslinked lysozyme dimer.

Crystal	Parent lysozyme	GA-modified monomer of lysozyme	GA-crosslinked dimer of lysozyme
Space group	$P4_32_12$	$P4_32_12$	$P4_32_12$
Unit cell parameters (Å)	$a=b=78.64$, $c=36.88$	$a=b=79.25$, $c=36.83$	$a=b=79.91$, $c=36.97$
Unit cell volume (Å^3)	228127.9	231289.6	236104.7
Resolution (Å)	42.2–1.42 (1.44–1.42)	50.0–1.08 (1.10–1.08)	50.0–1.46 (1.49–1.46)
No. of reflections	258,729	1,344,465	37,262
No. of unique reflections	22,456 (1,089)	50,765 (2,488)	21,467 (545)
Completeness (%)	99.9 (99.9)	99.9 (99.7)	68.4 (57.3)
Mosaicity (°)	0.36	0.21	0.98
R_{merge}[a]	0.023 (0.44)	0.054 (0.44)	0.073 (0.56)
I/σ (I)	90.9 (26.0)	82.26 (7.7)	18.5 (1.50)
Wilson B factor (Å^2)	14.96	7.10	16.06

[a]$R_{merge} = \sum hkl \sum i |Ii(hkl) - I(hkl)| / \sum hkl \sum i Ii(hkl)$, where $\sum hkl$ denotes the sum over all reflections and $\sum i$ the sum over all equivalent and symmetry-related reflections (Stout and Jensen, 1968).

modified, though not crosslinked, by polymeric glutaraldehyde (Fig. 6a), indicating a site-preferred point chemical mutation.

Crystallization of Glutaraldehyde-Crosslinked Dimers of Lysozyme

The crystallization conditions of the dimeric fraction of the crosslinked lysozyme was screened using Crystal Screen HT. Crystallization conditions consisting of 0.1 M bicine buffer pH 9.0 containing 2.0 M magnesium chloride hexahydrate yielded the envisaged crystal with the parameters and data collection statistics listed in Table III. This crystal belonged to the tetragonal system and its unit cell parameters were almost the same as those of its parent (native) lysozyme crystal. While noticeable intramolecular structural changes were not observed, analysis of electron-density maps

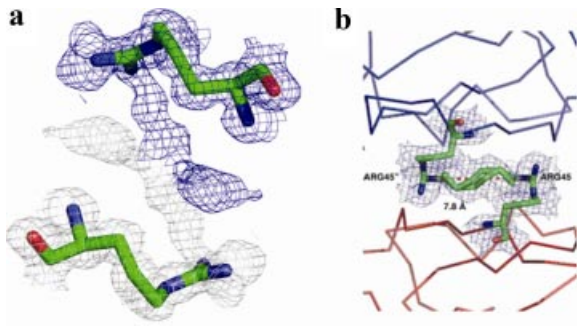

Figure 6. Part of the interface in the structure of (**a**) a glutaraldehyde-modified lysozyme monomeric crystal and (**b**) glutaraldehyde-crosslinked lysozyme dimeric crystal. Electron density is observed between Arg45 and the symmetrically related Arg45.

confirmed the presence of an intermolecular electron-density continuum between the Arg45–Arg45 pair (Fig. 6b), similar to that observed for the 10-min, 24, and 48-h time groups of the crosslinked lysozyme crystals, clearly indicating preservation of the relative orientation and chemical crosslinking identified in the pre-dissolved parent crystal.

Conclusion

We formulated a working hypothesis enabling us to extricate homogeneous populations of chemically modified single protein molecules or crosslinked protein dimers, and we demonstrated its feasibility on protein crystals crosslinked by glutaraldehyde. Potential applications of the homogeneous population of modified lysozyme monomer and crosslinked dimer thus obtained include oriented immobilization of single active lysozyme molecules and generation of hyperactive soluble lysozyme dimers. Our findings open the way to extending the proposed methodology to additional crosslinking agents and their mixtures, which are currently under investigation.

The authors are grateful to the Department of Biological Services, The Weizmann Institute of Science, Rehovot for their help with ESI-MS assay, and to the European Synchrotron Radiation Facility (ESRF, Grenoble, France) for synchrotron beam time. This research was supported by the Israel Science Foundation (ISF, grant no. 839/08). This work was supported in part by the Edouard Seroussi Chair for Protein Nano-Biotechnology.

References

Adams PD, Afonine PV, Bunkoczi G, Chen VB, Davis IW, Echols N, Headd JJ, Hung L-W, Kapral GJ, Grosse-Kunstleve RW, McCoy AJ, Moriarty NW, Oeffner R, Read RJ, Richardson DC, Richardson JS, Terwilliger TC, Zwart PH. 2010. PHENIX: A comprehensive Python-based system for macromolecular structure solution. Acta Crystallogr D Biol Crystallogr 66:213–221.

Cohen-Hadar N, Wine Y, Lagziel-Simis S, Moscovich-Dagan H, Dror Y, Frolow F, Freeman A. 2009. Protein crystal-mediated biotemplating. J Porous Media 12(3):213–220.

Cohen-Hadar N, Wine Y, Nachliel E, Huppert D, Gutman M, Frolow F, Freeman A. 2006. Monitoring the stability of crosslinked protein crystals biotemplates: A feasibility study. Biotechnol Bioeng 94(5):1005–1011.

Cosier J, Glazer AM. 1986. A nitrogen-gas-stream cryostat for general X-ray-diffraction studies. J Appl Crystallogr 19:105–107.

DeLano WL. 2002. The PyMol molecular graphics system. http://www.pymol.org.

Ducruix A, Giege R. 1999. Crystallization of nucleic acids and proteins: A practical approach. Oxford: Oxford Publishing Press.

Emsley P, Lohkamp B, Scott WG, Cowtan K. 2010. Features and development of Coot. Acta Crystallogr D Biol Crystallogr 66:486–501.

Giordano R, Leal RMF, Bourenkov GP, McSweeney S, Popov AN. 2012. The application of hierarchical cluster analysis to the selection of isomorphous crystals. Acta Crystallogr D Biol Crystallogr 68:649–658.

Guli M, Lambert EM, Li M, Mann S. 2010. Template-directed synthesis of nanoplasmonic arrays by intracrystalline metalization of cross-linked lysozyme crystals. Angew Chem Int Ed 49(3):520–523.

Kabsch W. 1993. Automatic processing of rotation diffraction data from crystals of initially unknown symmetry and cell constants. J Appl Crystallogr 26:795–800.

Kabsch W. 2010a. Integration, scaling, space-group assignment and post-refinement. Acta Crystallogr D Biol Crystallogr 66:133–144.

Kabsch W. 2010b. XDS. Acta Crystallogr D Biol Crystallogr 66:125–132.

Margolin AL, Navia MA. 2001. Protein crystals as novel catalytic materials. Angew Chem Int Ed 40(12):2205–2222.

Matthews BW. 1968. Solvent content of protein crystals. J Mol Biol 33(2): 491–497.

Migneault I, Dartiguenave C, Bertrand MJ, Waldron KC. 2004. Glutaraldehyde: Behavior in aqueous solution, reaction with proteins, and application to enzyme crosslinking. Biotechniques 37(5):790–802.

Nanjo F, Sakai K, Usui T. 1988. p-Nitrophenyl penta-*N*-acetyl-β chitopentanoside as a novel synthetic substrate for the colorimetric assay of lysozyme. J Biochem 104:255–258.

Otwinowski Z, Minor W. 1997. Processing of X-ray diffraction data collected in oscillation mode. Methods Enzymol 276:307–326.

Stout GH, Jensen LH. 1968. X-ray structure determination: A practical guide. London: Macmillan.

Teng TY. 1990. Mounting of crystals for macromolecular crystallography in a freestanding thin-film. J Appl Crystallogr 23:387–391.

Vilenchik LZ, Griffith JP, St Clair N, Navia MA, Margolin AL. 1998. Protein crystals as novel microporous materials. J Am Chem Soc 120(18):4290–4294.

Wine Y, Cohen-Hadar N, Freeman A, Frolow F. 2007. Elucidation of the mechanism and end products of glutaraldehyde crosslinking reaction by X-ray structure analysis. Biotechnol Bioeng 98(3):711–718.

Worthington. 1993. http:/www.worthington-biochem.com/LY/assay.html.

Zelinski T, Waldmann H. 1997. Cross-linked enzyme crystals (CLECs): Efficient and stable biocatalysts for preparative organic chemistry. Angew Chem Int Ed Engl 36(7):722–724.